

LuTan-1 InSAR Products Assessments for Geohazards and Geoinformation Monitoring

Tao Li¹, Xinming Tang², Xiang Zhang¹, Jing Lu¹, Xin Tian², Xuefei Zhang¹

¹ Land Satellite Remote Sensing Application Center, Ministry of Natural Resources, 100048, Beijing, China – rs_litao@163.com, zhangtaosas@qq.com, zhangx@lasac.cn, luj@lasac.cn, zhangxf@lasac.cn;

² Southeast University, 211189, Nanjing, China – tangxinming99@qq.com, tianxin@seu.edu.cn.

Keywords: LuTan-1, InSAR Application, Geohazard Monitoring, Geoinformation Production.

Abstract

LuTan-1 (LT-1) satellites have been launched for about 4 years. 771,282 images have been distributed to the users of China till 29th October, 2025. Main application purpose of LT-1 was geohazard monitoring and geoinformation production. Interferometric capability was the primary consideration for LT-1. In this paper, we assessed the interferometric applications in the natural resource monitoring industry. First, we overviewed the status of LT-1, the main interferometric products were introduced as S2A, S2B, S3A, S4A, S5A, S5B and S5C. They were geometrically calibrated single look complex (SLC) image, interferometrically calibrated SLC, differential interferometric synthetic aperture radar (SAR, InSAR, DInSAR) products, stacking, MTInSAR, digital orthorectified image, and digital surface model, respectively. S2A were generated after geometric calibration, the geometric accuracy was about 1.53 m after calibration. The baseline was then calibrated for helix bistatic formation data and generate S2B whose accuracy was better than 0.96 m. S3A, S4A and S5A were all used for deformation monitoring, the accuracy values of them were 2.7 mm, 8.6 mm/yr, and 3.7 mm. Geometric accuracy of S5B was 12.5 m, and the height accuracy of S5C was better than 4.7 m. More than 330 geohazards were detected in Guangdong province. The geohazards recognition rate in the field working stage increased from 28% to 47.24%. Even a prediction has been made to avoid disaster for a family and saved 3 people. The application effectiveness has been validated through those years.

1. Introduction

LuTan-1 (LT-1) A and B satellites were launched on 20220126 (YYYYMMDD) and 20220227 (Li et al. 2022). Four formations have been adopted since its launch. The first formation was the self-interferometric formation started at the launch of the first satellite. LT-1A started imaging on 20220209 and obtained its secondary image 8 days after. The first interferogram was highly coherent with perpendicular baseline of 46.7 m. LT-1B was launched with the orbital phase difference equal to 45 degrees compared to LT-1A. That was the second formation and the revisit time was equal to 1 day at fastest. At 20220525 LT-1B started to change the orbit to helix bistatic formation (HBF). That cost about 20 days and LT-1 started to collect the data for digital surface model (DSM) generation of China. We used the short baseline for three months and then convert to long baseline to collect most of the regions for more than two times. On 20230107, LT-1B converted to the fourth formation with the orbital phase difference equal to 180 degrees compared to LT-1A. That was the pursuit monostatic formation (PMF) which would last till the end of the life of LT-1. This was used to collect the deformation information all over China. We finished the in-orbit test before 20230401 and started to collect the data over China on 20240622 using stripmap 1 mode.

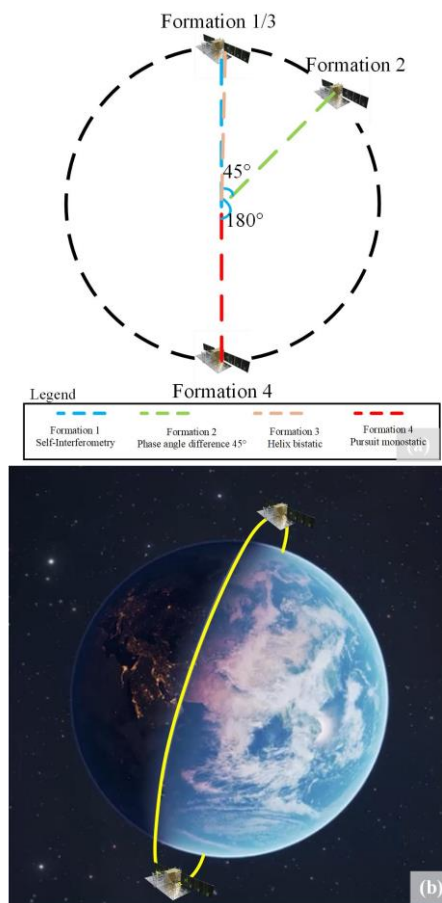


Fig. 1 (a) Four formations of LT-1 and (b) an example of pursuit monostatic formation (Tang et al. 2024).

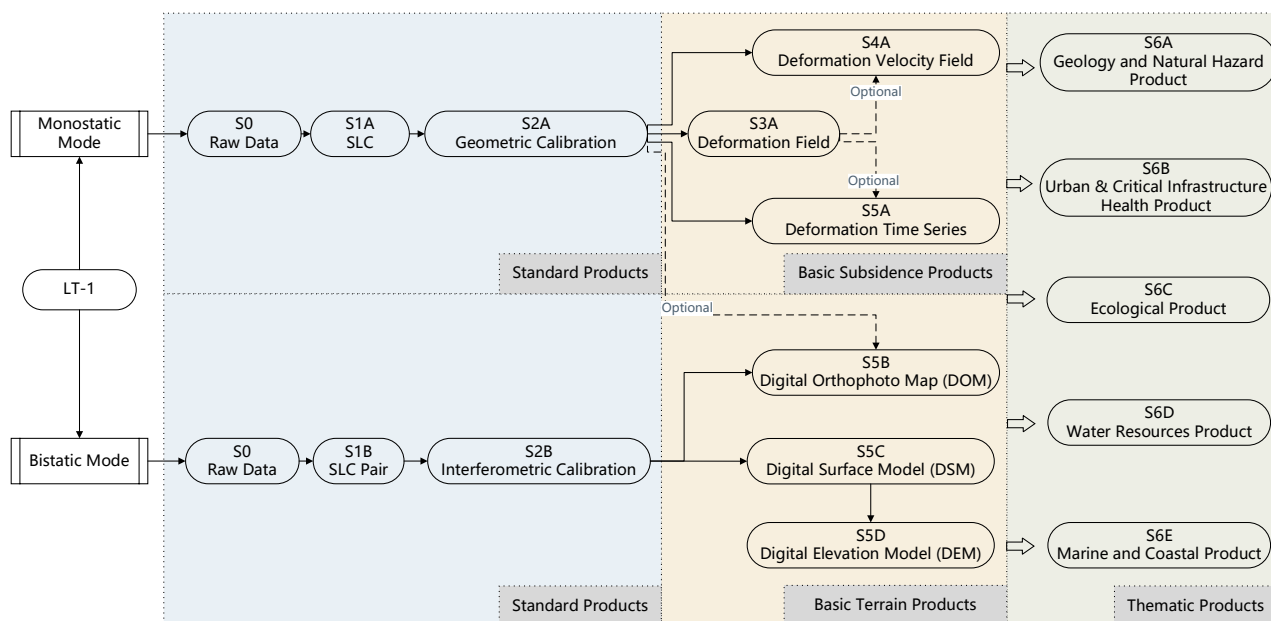


Fig. 2 Product system of LT-1.

Since 20251029, we have already collected 771,282 images. They were distributed to 32 provincial satellite remote sensing application centres to serve for the natural resources monitoring and supervision. In this paper, we introduced the interferometric products and applications of LT-1, see Fig. 1. LT-1 first adopted HBF to generate digital surface model (DSM) over the rainy and cloudy regions of China. Then the constellation converted to PMF to collect deformation information of Earth surface (Tang et al. 2025). DSM and deformation produced using interferometric information are the main products of LT-1. We concentrated in assessing the interferometric capability and the applicability of LT-1 in geoinformation collection and geohazards monitoring in this paper.

2. Interferometric Products

2.1 Products Definition

Interferometric products of LT-1 were designed following HBF and PMF (Li et al. 2023), see Fig. 2. The HBF provided DSM and DEM. The PMF provided deformation products. All the products were divided into three classes due to their processing stages. The first class is standard products. They were the data obtained and processed by the ground segment. The S0 was the raw data processed by receiving and decoding the signal downlinked from the satellite. S0 was not sent to the users. S1A and S1B were the single look complex (SLC) and SLC pairs, respectively. S1A was obtained using the PMF and no further processing is taken except the focusing, radiometric calibration and polarimetric calibration. S1B was obtained using the HBF. The SLC images after the aforementioned processing were co-registered and the baseline information were calculated to provide initial estimation. The geometric information and interferometric information of S1 was not accurate. Location error of S1A was about 40 m. And the baseline error of S1B was about 3 cm. This was not enough for further processing. Therefore, the data should be calibrated. After geometric calibration, we generated S2A and the location accuracy increased from 40 m to better than 4 m. The S2B data has been calibrated using the multi-interferometric beams of LT-1 and

the baseline accuracy increase to better than 1.2 cm. The calibrated data were distributed to the users for product generation.

The second class was basic products. They were the common products that can be further used by multiple industries. The basic deformation products consisted of S3A, S4A and S5A (Tao Li 2023). S3A was the deformation field product generated using DInSAR results. S4A was deformation velocity made from stacking. S5A was multi-temporal deformation generated using multi-temporal InSAR (MTInSAR) technology. The basic geoinformation products were S5B, S5C and S5D, i.e., digital orthophoto map (DOM), digital surface model (DSM) and digital elevation model (DEM), respectively.

The third class was thematic products. This was especially designed for the different industries. We only processed these products on demand. No operational processing was carried out for the thematic products.

2.2 Standard Products and Key Technologies

We constructed two kinds of calibration fields. The first was fixed calibration field. It contained 16 fixed corner reflectors (CR), see Fig. 3(a). Each CR was made of a reflective component, a driving component, and a solar panel as shown in Fig. 3(b). The pitch and azimuth angle of the CR could be adjusted by the control centre located at LASAC, MNR. The second were two mobile calibration fields with each contained 16 mobile CR, see Fig. 4(b). The calibration field and CRs could all be used to conduct geometric calibration.

Geometric calibration was carried out using the fixed CRs. We selected the corresponding pixels in the SLC images, the accuracy was around 1/1000 pixel, thus decreasing the pixel location error. A newly proposed method was used to improve the geometric accuracy. That was the beam related geometric calibration method which used the function to fit the azimuth clock deviation and the range time delay with the looking angle. This was based on the newly discovered error mechanism that the azimuth clock deviation was related to the beams, see Fig. 5. Each beam was provided with a correction to improve the

location accuracy. We monitor the geometric accuracy from the first geometric calibration task which was started on 20220712 to now, the geometric accuracy was 3.38 m for the worst. An average error of 1.53 m with standard deviation of 0.96 m was obtained, proving that the geometric accuracy and stability was high enough to generate S2A operationally.

Interferometric calibration was carried out using the mobile calibration fields. We have established the fields both in Shangqiu of Henan Province and Suqian of Jiangsu Province. The two fields were around 300 km far away from each other in the across track direction and 38 km in the along track direction. Shangqiu was located at the 4th beam of LT-1 and Suqian was the 11th, they were the smallest and biggest interferometric beam of LT-1. The distances between the two fields were able to separate the perpendicular and parallel baseline given the difference sensitivities of the two parameters to the height error, see Fig. 6. Error induced by parallel baseline error was about 60 times more than perpendicular baseline error. We firstly calculated the parallel baseline error by using the two calibration fields and CRs. Then the height error was minused and the perpendicular baseline error was calculated independently. The height accuracy values before and after interferometric calibration were 34.4 and 8.7 m. We used the ICESat-GLAS data to furtherly improve the accuracy to 2.6 m by removing the systematic errors(Song et al. 2024).

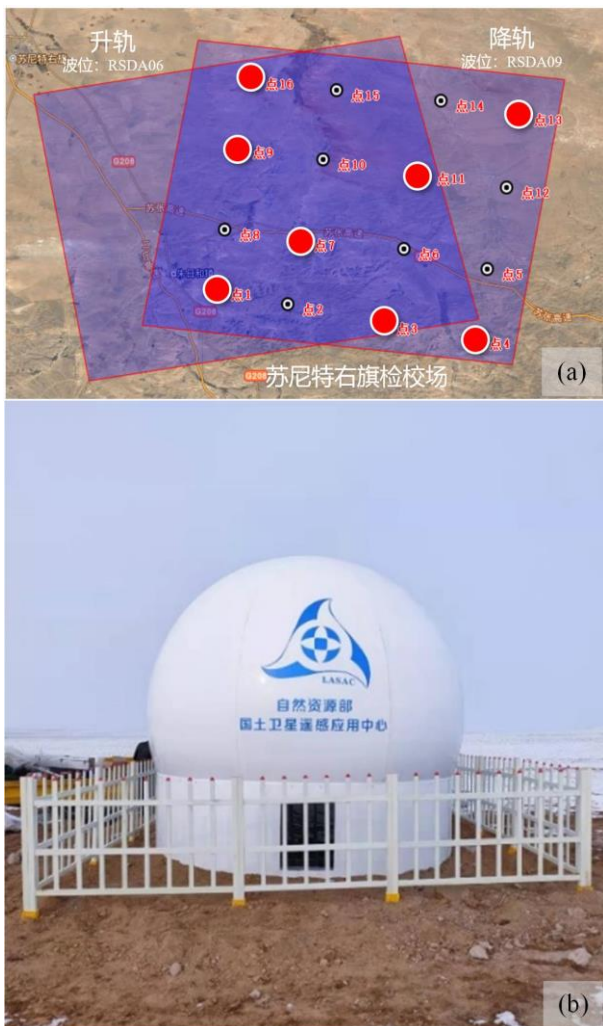


Fig. 3 (a)Fixed calibration field and (b)corner reflectors.

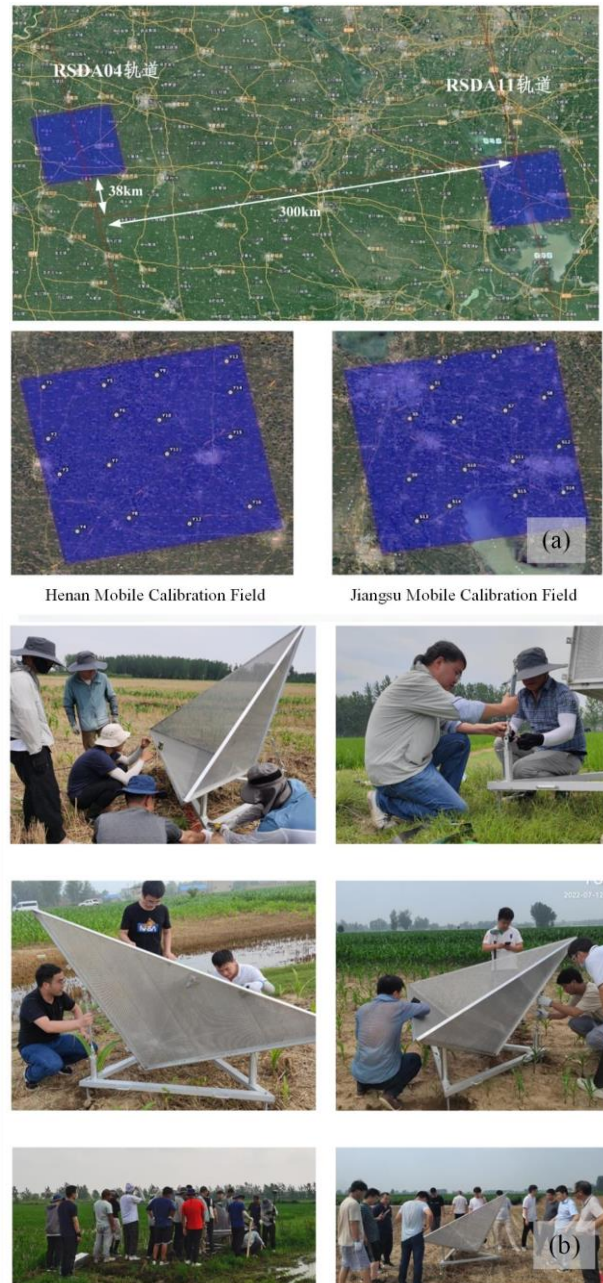


Fig. 4 (a)Mobile calibration fields and (b) corner reflectors.

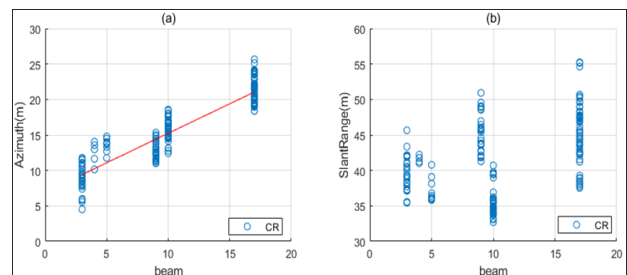


Fig. 5 (a) and (b) are the errors of the azimuth and slant range directions, respectively.

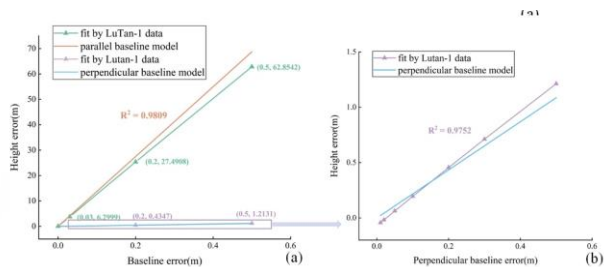


Fig. 6. Sensitivities of (a) perpendicular and parallel baseline errors to height error and (b) perpendicular baseline error to height error.

2.3 Basic Products and Key Technologies.

2.3.1 Basic Deformation Products: DInSAR was the easiest way to provide deformation information. The processing procedures were relatively consensus. We used the common method but added the general atmospheric correction online system (GACOS) model (Xiao et al. 2021) developed especially for LT-1. Then the DInSAR results were mosaiced by using the least square estimation method which link the common points in the overlap regions of the neighbouring images.

Stacking was more stable than DInSAR because the random errors have been decreased during the processing. The errors included the atmospheric residues, the orbital error, the terrain residues, the random noises. Stacking provided the internal accuracy estimation method during least square estimation. The users were able to assess the quality of S4A themselves using the internal accuracy.

MTInSAR was relatively complicated because many processing methods have been proposed. In our processing, we selected the common processing procedures including persistent scatterer (PS) selection, networking, relative parameter calculation along arcs, least square estimation, and finally the nonlinear phase components decomposition.

We processed S3A operationally. About 800 images were processed every day. The whole S3A products of China were updated every 28 days. S4A and S5A were processed on demand. The typical results of S3A over China, S4A over Shaanxi and S5A over Henan were shown in Fig. 7. To assess the deformation accuracy of LT-1, we collected the levelling data every 4 days when the satellite revisited the same place of Yungang District, Datong City, Shanxi Province during in-orbit test phase. Root-mean-square-error (RMSE) of S3A, S4A and S5A were around 2.7 mm, 8.6 mm/yr, and 3.7 mm.

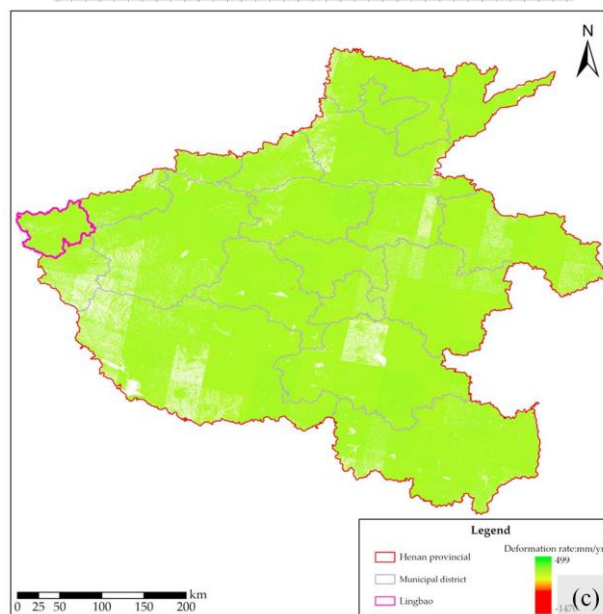
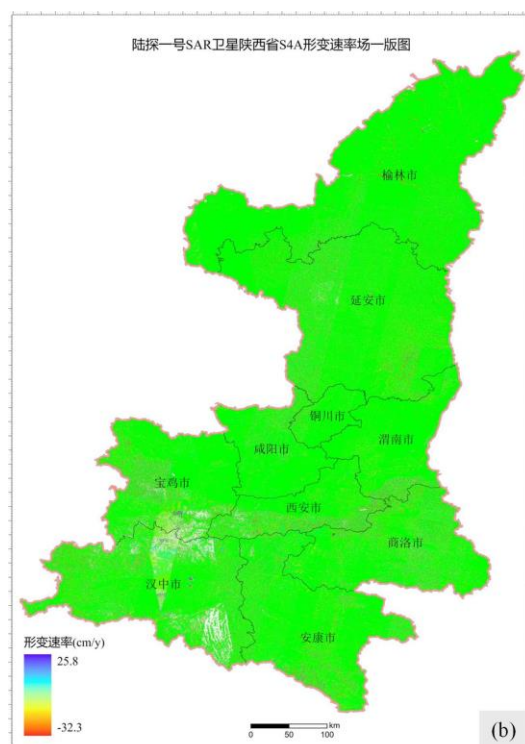
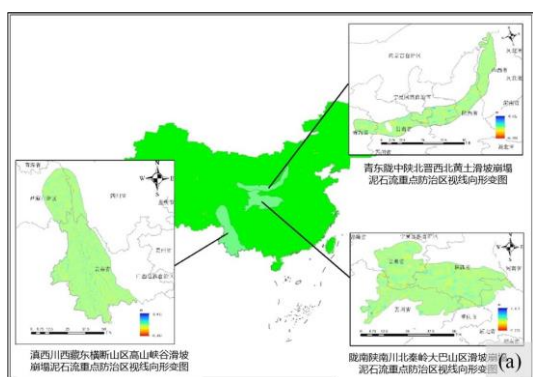


Fig. 7 Deformation products. (a) is S3A of China. (b) is S4A of Shaanxi Province. (c) is S5A of Henan Province.

2.3.2 Basic Geoinformation Products: S5B was generated using the SLC image and external DEM on demand. We had generated the product of China using the stripmap 2 images collected in 2022, see Fig. 8(a). The products were assessed using 158 feature points over China, the RMSE was less than 12.5 m.

S5C was generated following the standard processing chains of InSAR. We have divided the processing chains into two parts, i.e., the standard processing to generate raw DSM, and the mosaic processing to generate DSM of wide area. We defined the accuracy according to the different terrain types, i.e., flat region, hilly region and mountainous region. The accuracy



values of the data over pre-selected regions of Jiangsu, Shaanxi, and Sichuan were 1.2 m, 1.6 m and 4.7 m, respectively.

S5D was generated by editing the S5C product. The artificials and the forest should be removed and the rivers should be filled with the surrounding elevation values. We did not produce S5D unless there were business requirements.

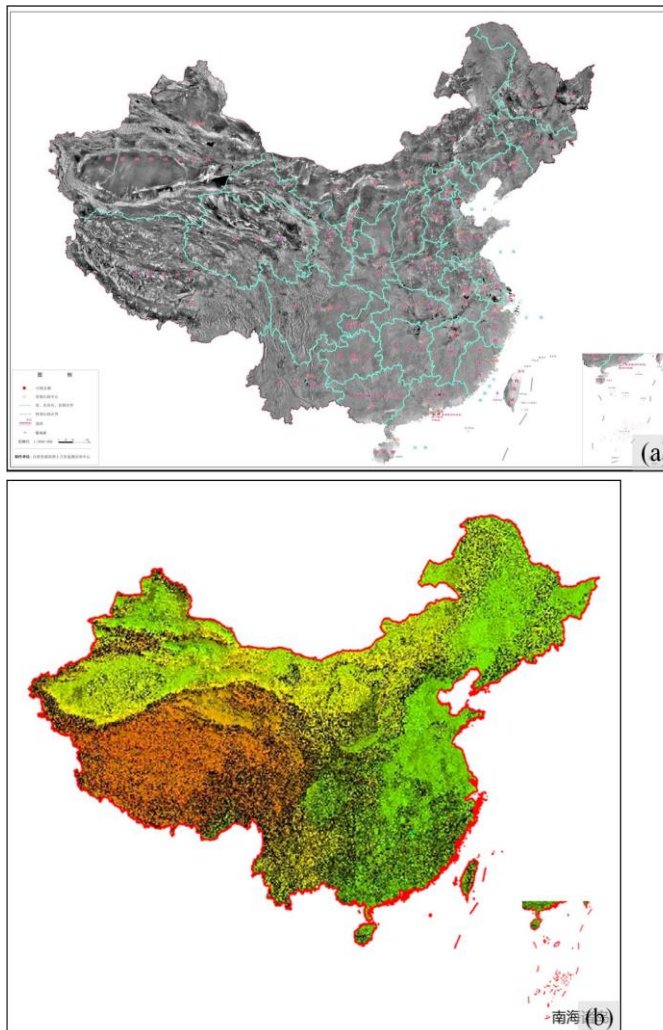


Fig. 8 (a) Digital orthorectified map and (b) digital elevation model of China.

2.4 Software and Systems

LandSAR was the software used to process the LT-1 data. It was especially designed for LT-1 to fit the minor problems that may be encountered during the processing of the first China interferometric SAR satellite. The software was compatible with partial loss of GNSS data, co-registration with different pulse repetition frequency, stacking with different image coverages, et. al. The software was now used by more than 100 of organizations. The introduction of LandSAR could be found on the website along with its example data (LASAC and BSIT 2023).

The processing system was designed according to the functions of LandSAR. The system was now supporting the operational processing of S2A and S3A. S2A was processed and distributed totally automatically. Nearly 800 images were processed every day. S3A was processed without people but only distributed on

demand. The temporal baseline of S3A was set to 100 days, meaning that each image was combined with two earlier images, therefore about 1600 DInSAR products were produced every day.

3. Applications

There were three primary users of LT-1. They were the Ministry of Natural Resources (MNR), the Ministry of Emergency Management (MEM), and the National Forestry and Grassland Administration. The interferometric productions were mainly used by the MNR and MEM.

The basic deformation products have been used in the national geohazards identification by MNR. 4,120, 000 km² regions with high and medium geohazard susceptibility have been covered. Provinces of Shaanxi, Henan, Guizhou, Sichuan and Shandong have conducted the deformation monitoring of the whole provincial regions. Among them Shaanxi have conducted more than 10 times for the geohazard monitoring by jointly using the InSAR and optical images over the whole province. More than 379 potential geohazards have been identified. Those regions covered 65 counties of 10 cities. 354 potential geohazards have been investigated by field working and 83 have been recognized as geohazards. The geohazards recognition rate in the field working stage increased from 28% to 47.24%. Henan identified more than 1300 deformation regions. Shandong identified more than 1000 deformation regions in 2024. Guangdong have found 330 potential geohazards. There was a potential geohazard located at the Xiapingsha Village of Dapu County, Meizhou City of Guangdong Province on 17th August, 2024. The field working staff have transferred the villagers, thus avoiding the injuries and deaths of the family when the landslide collapsed on 20th August, 2024.

The basic deformation products have been used by the MEM for earthquake monitoring. Since 2022, the data have been used in Sichuan Luding Earthquake, Gansu Jishishan Earthquake, Turkey Earthquake, Xizang Rikaza Earthquake, et al. The fastest corresponding time was only several hours.

4. Conclusions

LT-1 was the first L-band interferometric satellite constellation for China. Since their launch on 26th January and 27th February 2022, more than 771,282 SLC images have been sent to 32 provincial satellite remote sensing application centres of China. The DSM data have been collected in most China for at least one time and in some regions more than 3 times by combining the descending-ascending and long-short-baseline observations. The DInSAR data have been collected all over China since 22nd June 2023 regularly each 28 days. Till now most of China regions have been covered for 29 times. Now we are developing the processing systems for stacking and MTInSAR to generate S4A and S5A operationally. Accuracies that we obtained till now were shown in Tab.1.

Products	Brief Introduction	Accuracy
S2A	Geometrically calibrated	1.53 m
S2B	Interferometrically calibrated	0.96 m
S3A	DInSAR	2.7 mm
S4A	Stacking	8.6 mm/yr
S5A	MTInSAR	3.7 mm
S3B	DSM	4.7 m

Table 1. Products accuracies.

Besides the products, LandSAR software and the processing chains have already provided accordingly to help most of the users with the application of the LT-1 data. The software has been sent to more than 100 users for free trial. Meantime, the processing chains have been established for the Shaanxi Satellite Application Technology Centre and the Geological Environment Monitoring Institute of China Geological Survey and operational processing of S3A have been taken by the two organizations.

LT-1 have made a milestone for China remote sensing research. However, there are also some problems waiting to solve. First of all, SAR satellites are not sensitive to the deformation in North-South directions. Secondly, the coverage time is too long to be used for disaster prediction. Although the orbital revisiting time is only 4 days for LT-1A/B, 28 days have to be cost to cover the whole China regions using 7 interferometric beams. We need to use the high-resolution-wide-swath technology to increase the data collection capacities and increase the data down-linking capability. Thirdly, L band is not enough to observe the deformation of buildings. Satellites with shorter wavelength should be considered for more elaborate deformation monitoring.

Acknowledgements

The authors would like to thank the Natural Resources Shaanxi Satellite Application Technology Centre, Henan Provincial Geological Bureau for their data processing and sharing.

References

LASAC, & BSIT (2023). The interferometric SAR processing software: LandSAR. In <http://sasclouds.com/chinese/applicationExtend/software/LandSAR>.

Li, T., Tang, X., Gao, X., Zhang, Z., Zhang, X., Lu, J., Chen, T., Qiao, X., Han, J., & Li, Z. (2023). LuTan-1 SAR Satellite Characteristics and Productions in the Phase of In-Orbit Test. In *ISPRS GSW 2023*. Carlo, Egypt.

Li, T., Tang, X., Zhou, X., & Zhang, X. (2022). LuTan-1 SAR Main Applications and Products. In *EUSAR 2022*. Leipzig, Germany.

Song, X., Zhang, L., Li, T., Lei, B., & Song, R. (2024). Baseline refinement and DEM accuracy analysis during the in-orbit test phase of LT-1 SAR. *Acta Geodaetica et Cartographica Sinica*, 53, 1920-1929.

Tang, X., Li, T., Chen, J., Wei, C., Zhang, X., Liu, Y., Liu, D., Zhang, X., Zhou, X., Lu, J., Yue, Q., Liu, K., & Wang, R. (2025). Twin-Satellite Constellation Design and Realization for Terrain Mapping and Deformation Monitoring: LuTan-1. *IEEE Transactions on Geosciences and Remote Sensing*, 63, 1-14.

Tang, X., Li, T., Zhang, X., Zhou, X., Lu, J., & Zhang, X. (2024). In-orbit application parameters test and analysis of L-band differential interferometric SAR satellite constellation. *Acta Geodaetica et Cartographica Sinica*, 53, 1863-1872.

Li, T, Tang, X., Li, S., Zhou X., Zhang X., Xu Y.(2023). Classification of basic deformation products of L-band differential interferometric SAR satellite. *Acta Geodaetica et Cartographica Sinica*, 52, 769-779.

Xiao, R., Yu, C., Li, Z., & He, X. (2021). Statistical assessment metrics for InSAR atmospheric correction: Applications to generic atmospheric correction online service for InSAR (GACOS) in Eastern China. *International Journal of Applied Earth Observation and Geoinformation*, 96, 102289.